Available online at www.sciencedirect.com
ScienceDirect
Biochimica et Biophysica Acta 1758 (2006) 1426–1435
BIOCHIMICA ET BIOPHYSICA ACTA
BBA
www.elsevier.com/locate/bbamem

Influence of N-acylation of a peptide derived from human lactoferricin on membrane selectivity

Dagmar Zweytick [a], Georg Pabst [a], Peter M. Abuja [a], Alexander Jilek [a,1], Sylvie E. Blondelle [b], Jörg Andrä [c], Roman Jerala [d], Daniel Monreal [e], Guillermo Martinez de Tejada [e], Karl Lohner [a,*]

[a] *Institute of Biophysics and X-ray Structure Research, Austrian Academy of Sciences, Schmiedlstraße 6, A-8042 Graz, Austria*
[b] *Torrey Pines Institute for Molecular Studies, 3550 General Atomics Ct, San Diego, CA 92121, USA*
[c] *Division of Biophysics, Research Center Borstel, Leibniz-Center for Medicine and Biosciences, Parkallee 10, D-23845 Borstel, Germany*
[d] *National Institute of Chemistry, Laboratory for Biotechnology, Hajdrihova 19, SI-1000 Ljubljana, Slovenia*
[e] *Departamento de Microbiología Universidad de Navarra, 31080 Pamplona, Spain*

Received 18 January 2006; received in revised form 16 February 2006; accepted 16 February 2006
Available online 27 March 2006

Abstract

Increasing numbers of bacterial strains being resistant to conventional antibiotics emphasize the urgent need for new antimicrobial agents. One strategy is based on host defence peptides that can be found in every organism including humans. We have studied the antimicrobial peptide LF11, derived from the pepsin cleavage product of human lactoferrin, known for its antimicrobial and lipid A-binding activity, and peptide C12LF11, the N-lauryl-derivative of LF11, which has owing to the attached hydrocarbon chain an additional hydrophobic segment. The influence of this hydrocarbon chain on membrane selectivity was studied using model membranes composed of dipalmitoylphosphatidylglycerol (DPPG), mimicking bacterial plasma membranes, and of dipalmitoylphosphatidylcholine (DPPC), a model system for mammalian membranes. A variety of biophysical techniques was applied. Thereby, we found that LF11 did not affect DPPC bilayers and showed only moderate effects on DPPG membranes in accordance with its non-hemolytic and weak antimicrobial activity. In contrast, the introduction of the N-lauryl group caused significant changes in the phase behaviour and lipid chain packing in both model membrane systems. These findings correlate with the in vitro tests on methicillin resistant *S. aureus*, *E. coli*, *P. aeruginosa* and human red blood cells, showing increased biological activity of C12LF11 towards these test organisms. This provides evidence that both electrostatic and hydrophobic interactions are crucial for biological activity of antimicrobial peptides, whereas a certain balance between the two components has to be kept, in order not to loose the specificity for bacterial membranes.

Keywords: Acylation and antimicrobial peptide; Lactoferrin; Antimicrobial and hemolytic activity; Model membrane

1. Introduction

Growing concern about the increase of bacterial strains being resistant against conventional antibiotics has spurred research on alternative agents, in particular on peptide antibiotics, which play an important role in the innate immune system [1–4]. These peptides are characterized by amphipathic structures, which are often formed only during their contact with membranes. They are cationic, a property that is believed to form the basis for their partial or complete selectivity against negatively charged bacterial membranes [5–8]. Furthermore, studies on e.g. pardaxin, which exhibits antimicrobial activity and is toxic at high concentrations, indicated that peptides may exert different membrane disrupting mechanisms depending on the lipid composition [9]. Considering the diversity of lipids in cell membranes, it may not be too surprising that different mechanisms of action have evolved in nature [10]. Thus, one major issue in the quest for novel peptide antibiotics is to find peptides with high activity against prokaryotic cells and low toxicity towards eukaryotic cells. While many such peptides

* Corresponding author. Tel.: +43 316 4120 323; fax: +43 316 4120 390.
E-mail address: Karl.Lohner@oeaw.ac.at (K. Lohner).
[1] Present address: Institute of Organic Chemistry, University of Linz, Altenbergstrasse 60, A-4040 Linz, Austria.

0005-2736/$ - see front matter © 2006 Elsevier B.V. All rights reserved.
doi:10.1016/j.bbamem.2006.02.032

have been identified, their molecular mode of action against bacteria remains so far largely unclear [10].

One example of naturally occurring antimicrobial peptides is lactoferricin (LFcin) [11,12]. LFcin is a pepsin cleavage fragment from lactoferrin (LF), a multifunctional iron-binding glycoprotein originally discovered in bovine milk [13] and later in exocrine secretions of mammals, as well as in granules and neutrophils during inflammatory responses [14,15]. Bovine LFcin contains a region that forms an amphipathic α-helix, but when isolated, this peptide fragment folds into a β-hairpin structure [16,17]. Human lactoferricin (hLFcin) comprises amino acid residues 1–45 of the N-terminus of human lactoferrin (hLF) and has enhanced antibacterial activity as compared to intact hLF [18]. Unlike bovine LFcin the longer hLFcin displays a nascent helical structure (Gln14–Lys29) that is better stabilized in membrane mimetic systems [19]. LFcin inhibits growth of a diverse range of microorganisms like Gram-negative bacteria, Gram-positive bacteria, and yeast filamentous fungi, including some antibiotic resistant pathogens [20]. It is supposed to kill the target organisms by membrane permeabilization and suppresses the activation of innate immunity by microbial components such as lipopolysaccharides [20]. To help identify the 'antimicrobial principle' in LF, derivatives have been constructed and a wealth of data have been collected to gain insight into the mode of antibacterial action of LF [12,17]. Furthermore, it was shown in particular for helical peptides that antimicrobial activity is not only controlled by the overall charge but also by the hydrophobicity of the peptides [21–23]. Therefore one of the strategies to improve antimicrobial activity may be the attachment of a hydrophobic chain that can compensate for lack of hydrophobicity [24]. In fact, Wakabayashi et al. [20,25] and Strom et al. [26] have shown that N-acylation of derivatives based on a sequence of bovine lactoferricin B (amino acids 17–41) resulted in higher antibacterial activity. However, such strategy usually leads to a higher toxicity towards eukaryotic cells, thus resulting in loss of target cell selectivity [24,27].

Therefore, we studied the effect of both LF11, an 11-residue fragment of hLF, and its N-lauryl-derivative, C12LF11, on membrane mimetic systems in order to gain information on the role of hydrophobic attachment for membrane selectivity. These peptides were selected based on previous studies demonstrating that the insertion of a 12 hydrocarbon chain at the C-terminal or N-terminal region of LF11 leads to the strongest enhancement in antibacterial activity and binding of lipopolysaccharide [28,29], therefore improving its potential therapeutic use to combat the harmful effects of sepsis [30]. The 11 amino acid stretching peptide LF11 comprises amino acid 21–31 of hLF, whereas methionine at position seven has been exchanged by an isoleucine to prevent oxidation.

Cell membranes contain a variety of lipid classes but depending on the species a common pattern can be seen: The cytoplasmic membrane of Gram-negative bacteria consists mainly of PE (phosphatidylethanolamine), PG (phosphatidylglycerol) and CL (cardiolipin), while Gram-positive bacteria have a large amount of PG and derivatives in their lipid bilayer membrane [7]. The plasma membrane of red blood cells, in turn, is comprised to a large amount (60%) of phospholipids and about 25% of cholesterol. Choline phosphatides (PC (phosphatidylcholine) and SM (sphingomyelin)) are the main components of the outer leaflet of mammalian red blood cell plasma membranes [7]. Accordingly, we have selected negatively charged 1,2-dipalmitoylphosphatidylglycerol (DPPG) as a model membrane system for bacterial membranes and 1,2-dipalmitoylphosphatidylcholine (DPPC) to mimic mammalian plasma membranes.

2. Materials and methods

2.1. Reagents

1,2-Dipalmitoylphosphatidylglycerol (Na-salt) (DPPG) and 1,2- dipalmitoylphosphatidylcholine (DPPC) were purchased from Avanti Polar Lipids, Inc. (USA), and used without further purification. Purity (>99%) was checked before and after experiments by thin layer chromatography showing a single spot using $CHCl_3/CH_3OH/NH_3$ (25% in water) (65:25:5, v/v) as mobile phase and detection with a phosphorus-sensitive reagent (molybdenic acid, [31]). Stock solutions of DPPC were prepared in $CHCl_3/CH_3OH$ (2:1, v/v), while DPPG was dissolved in $CHCl_3/CH_3OH/H_2O$ (9:1:0.01, v/v) and stored at −18 °C.

The peptides, LF11 (FQWQRNIRKVR-NH_2, M=1529.8 g/mol) and its N-lauryl derivative (C12LF11, (CH_3-$(CH_2)_{10}$-CO-NH-FQWQRNIRKVR-NH_2, M=1712.1 g/mol) were purchased from NeoMPS, Inc. (San Diego, CA, USA). The purities were >96% as determined by RP-HPLC. LF11 was dissolved in phosphate buffered saline (PBS, 20 mM NaPi, 130 mM NaCl, pH 7.4) at a concentration of 3 mg/ml. C12LF11 was dissolved in $CHCl_3/CH_3OH$ (1:2, v/v) at a concentration of 1 mg/ml. The peptide solutions were prepared freshly for each experiment.

2.2. Assays for antimicrobial and hemolytic activity

Antimicrobial activity of the peptides was tested using susceptibility microdilution assays according to NCCLS (National Committee for Clinical Laboratory Standards) approved guidelines. Briefly, a suspension of log-phase bacteria in Mueller–Hinton broth was added to serial dilutions of the peptide solution in microtiter plates that were subsequently incubated overnight at 37 °C. The bacterial growth was monitored to determine the minimal inhibitory concentration, MIC [32].

The hemolytic activity towards human red blood cells, which were obtained from heparinized human blood, was determined by the release of haemoglobin following an hour incubation at 37 °C [32]. Total release of haemoglobin was achieved by adding Triton X-100 (0.5% final concentration).

2.3. Preparation of liposomes

Appropriate amounts of the phospholipid stock solutions were dried under a stream of nitrogen and stored in vacuum overnight to completely remove organic solvents. The dry lipid film was then dispersed in PBS-buffer (or 20 mM HEPES, pH 7.0 for FTIR experiments) and hydrated at a temperature well above the gel to fluid phase transition of the respective phospholipid under intermittent vigorous vortex-mixing following a protocol depending on the respective phospholipid. The lipid concentration was 0.1 wt.% for calorimetric and fluorescence spectroscopy experiments, 1.5 wt.% for FTIR spectroscopy and 5 wt.% for the X-ray measurements. LF11 was added to the dry lipid film together with PBS at a lipid to peptide molar ratio of 25:1, while C12LF11 was dissolved in organic solvent and added at the same molar lipid to peptide ratio before drying the lipid. Identical hydration protocols were applied for liposomes with and without peptide. The fully hydrated samples were stored at room temperature until measurement (maximum up to 2 h).

2.4. Differential scanning calorimetry (DSC)

DSC experiments were performed with a differential scanning calorimeter (VP-DSC), from MicroCal, Inc. (Northampton, MA, USA). Samples were degassed before measuring. Heating scans were performed at a scan rate of 30 °C/h with a final temperature approximately 10 °C above the main transition temperature (T_m) and cooling scans at the same scan rate with a final temperature about 20 °C below T_m. The heating/cooling cycle was repeated twice, pre-scan thermostating was allowed for 15 min for the heating scans and 1 min for the cooling scans. Enthalpies were calculated by integrating the peak areas after normalization to phospholipid concentration and baseline adjustment using the MicroCal Origin software (VP-DSC version).

2.5. Small- and wide-angle X-ray scattering (SWAXS)

X-ray scattering experiments were performed on a SWAX-camera (HECUS X-ray systems, Graz, Austria) allowing simultaneous recording of diffraction data in both the small and the wide-angle region [33], which was mounted on a rotating-Cu-anode X-ray generator (Rigaku-Denki) operating at 4 kW. CuK_α-radiation ($\lambda = 1.542$ Å) was selected using a Ni-filter in combination with a pulse height discriminator. The camera was equipped with a Peltier-controlled variable-temperature cuvette (temperature resolution 0.1 °C) and two linear one-dimensional position-sensitive detectors OED 50-M covering both small and wide angle, regimes of interest. Calibration of the small-angle X-ray scattering (SAXS) patterns was performed with silver stearate, *p*-Br benzoic acid and Lupolen (solid polyethylene) were used to calibrate the wide-angle X-ray scattering (WAXS) patterns. A programmable temperature and time controller (HECUS X-ray systems, Graz, Austria) was used for temperature control and data acquisition. After equilibration of the samples for 10 min at the respective temperature, diffractograms for the small-angle region were recorded with total exposure times of 7200 s for the small angle regime and of 1800 s for the wide-angle region.

The phosphate–phosphate-distance, d_{pp}, was derived from the SAXS patterns using a global analysis technique described by Pabst et al. [34,35], where the paracrystalline theory was applied for those gel phase patterns that exhibited Bragg reflections. The domain size was calculated as product of the *d*-spacing (d) and the average number of lamellae (N_{mean}) obtained from the global fit.

2.6. FTIR spectroscopy

The infrared spectroscopic measurements were performed on an IFS-55 spectrometer (Bruker, Karlsruhe, Germany). The samples were placed in a CaF_2 cuvette with a 12.5 μm teflon spacer. Temperature-scans were performed automatically between 10 and 70 °C with a heating-rate of 0.6 °C/min. Every 1–3 min, 50 interferograms were accumulated, apodized, Fourier-transformed, and converted into absorbance spectra. For strong absorption bands, the band parameters (i.e., peak position, band width, and intensity) were evaluated from the original spectra, if necessary after subtraction of the strong water bands.

2.7. Fluorescence spectroscopy

Fluorescence spectroscopy experiments were performed using a SPEX Fluoro Max-3 spectrofluorimeter (Jobin-Yvon, Longjumeau, France) and spectra were analysed with the Datamax software. Tryptophan fluorescence spectra were obtained at room temperature (25 °C) using an excitation wavelength of 282 nm and a slit width of 5 nm for both excitation and emission monochromators. Peptides were diluted to 20 μg/ml in pure PBS or PBS containing the respective phospholipids as unilamellar liposomes at a lipid to peptide molar ratio of 25:1.

Quenching of Trp was carried out in the presence and absence of phospholipid liposomes using 0.1, 0.4 and 0.7 M acrylamide. The data were analyzed according to the Stern–Volmer equation [36]:

$$F_0/F = 1 + K_{SV}[Q]$$

where F_0 and F represent the fluorescence emission intensities in the absence and presence of the quencher molecule (Q), respectively, and K_{SV} is the collision Stern–Volmer quenching constant, which is a quantitative measure for the accessibility of tryptophan to acrylamide [37].

2.8. Optical microscopy

Phase contrast microscopy was performed on an inverted microscope equipped with Zeiss Plan-Neofluars, Ph 40× and 63× oil, respectively. Diluted samples were placed into a custom made specimen chamber that could be thermostated and was made of stainless steel with a glass window of 0.16 mm thickness and an optical path length of 2 mm within the sample.

3. Results

3.1. Biological activity

Representative results on the antimicrobial activities of both LF11 and C12LF11 towards prominent Gram-positive (methicillin-resistant *Staphylococcus aureus*, *MRSA* ATTC 33591) and Gram-negative bacterial strains (*Escherichia coli* ATCC 25922, and *Pseudomonas aeruginosa ATCC 27853*, respectively) are given in Table 1. LF11 exhibited no substantial antimicrobial activity and no hemolytic activity under the experimental conditions. In contrast, addition of the acyl chain to the N-terminal part of LF11 was found to strongly increase the antimicrobial activity towards all bacterial strains tested. Strong hemolytic activity was found at 100 μg/ml of peptide when tested under stringent conditions (i.e. 0.25% of human red blood cells in the hemolysis assay). This shows that the acylated peptide is able to interact also with mammalian membranes.

3.2. Differential scanning calorimetry of bacterial and mammalian model membranes

To correlate the variations in biological activities with the interaction of LF11 and C12LF11 with membranes two liposome systems were used: DPPG, which represents the negatively charged component of bacterial cytoplasmic membranes and DPPC, a zwitterionic component, typical of mammalian plasma membranes.

In agreement with published data [38,39], the temperature-dependence of the excess heat capacity of pure DPPG showed two phase transitions (Fig. 1), which can be attributed to the pre-transition from the lamellar-gel (L_β') to the ripple-phase (P_β') at 32.8 °C and the main or chain-melting transition from the P_β to the fluid (L_α) phase at 40.2 °C. Addition of LF11 (25:1 lipid to peptide molar ratio) resulted in a strong decrease of the pre-transition enthalpy (ΔH_{pre}) of DPPG (Fig. 1 and Table 2), whereas the main transition was unaffected. In contrast, addition of C12LF11 (25:1 lipid to peptide molar ratio) did not only abolish the pre-transition but had also a

Table 1
Minimal inhibitory concentration (MIC) of LF11 and C12LF11 (μg/ml)

Peptide	*MRSA* ATCC 33591	*E. coli* ATCC 25922	*P. aeruginosa* ATCC 27853
LF11	>250	256	>500
C12LF11	62	64	62

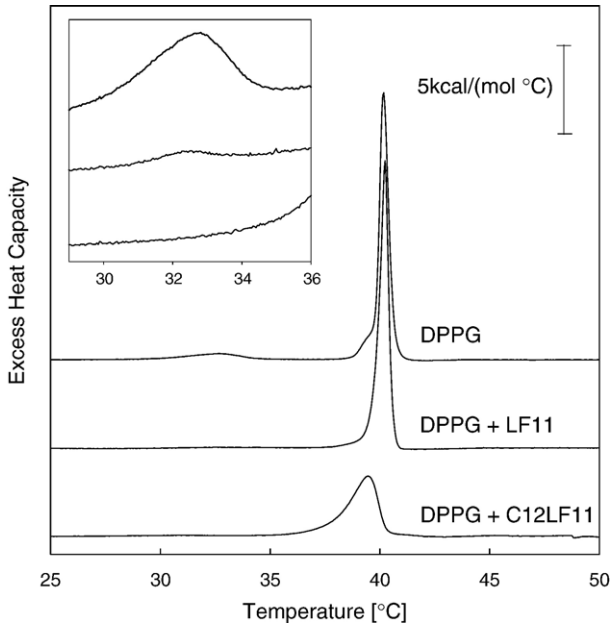

Fig. 1. DSC thermograms of DPPG in the absence and presence of LF11 or C12LF11 (25:1, lipid to peptide molar ratio). For clarity, the DSC curves were displayed on the ordinate by an arbitrary increment. The pre-transition is shown enlarged in the inset. Scan rate was 30 °C/h.

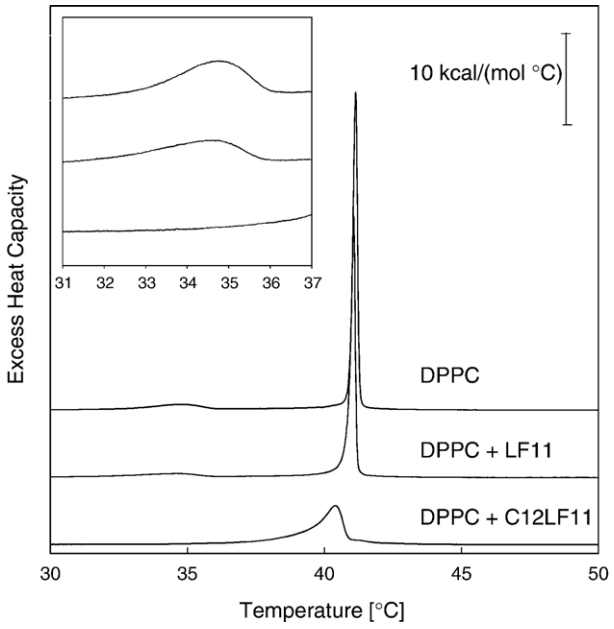

Fig. 2. DSC thermograms of DPPC in the absence and in the presence of LF11 or C12LF11 (25:1, lipid to peptide molar ratio). For clarity, the DSC curves were displaced on the ordinate by arbitrary units. The pre-transition is shown enlarged in the inset. Scan rate was 30 °C/h.

strong effect on the main transition enthalpy of DPPG (ΔH_m). In addition, a decrease in melting cooperativity was observed in the presence of C12LF11 as indicated by the increased transition half-width ($\Delta T_{1/2}$), as well as a destabilization of the gel phase as indicated by a lower main transition temperature (T_m) (Table 2).

The excess heat capacity curve of pure DPPC showed two transitions (Fig. 2), which can be attributed to the pre-transition at 34.8 °C and the main transition at 41.1 °C (Table 2), in agreement with published data [40]. In contrast to DPPG, addition of LF11 to DPPC (25:1 lipid to peptide molar ratio, Fig. 2) only showed a slight reduction of ΔH_{pre}. On the other hand, similar effects as in DPPG were observed upon addition of C12LF11 (1:25, Fig. 2), i.e., suppression of the pre-transition and a marked decrease of both ΔH_m and T_m as well as a strong increase of $\Delta T_{1/2}$ (Table 2).

3.3. Small and wide angle X-ray scattering

The small-angle X-ray scattering pattern of DPPG liposomes in the absence of peptides in the $L_{\beta'}$ phase (25 °C, i.e., below the pre-transition temperature) shows three weak lamellar diffraction orders with a lattice spacing d=118 Å, indicating a highly swollen lamellar system (Fig. 3). Compared to multilamellar dispersions of DPPC, the Bragg peaks are very broad and the scattering domain size of 470 Å shows that under these experimental conditions DPPG forms oligolamellar vesicles (N_{mean} ~ 4) within which the bilayers are positionally only

Table 2
Thermodynamic data of phospholipid phase transitions in the absence and presence of LF11 and C12LF11 at a lipid to peptide molar ratio of 25:1

	ΔH_{pre} (kcal/mol)	T_{pre} (°C)	ΔH_m (kcal/mol)	T_m (°C)	$\Delta T_{1/2}$ (°C)
DPPG	1.5	32.8	9.9	40.2	0.46
+LF11	0.2	32.9	10.4	40.2	0.46
+C12LF11	0	–	7.6	39.5	1.56
DPPC	1.7	34.8	8.8	41.1	0.18
+LF11	1.4	34.7	8.1	41.1	0.18
+C12LF11	0	–	6.4	40.4	1.01

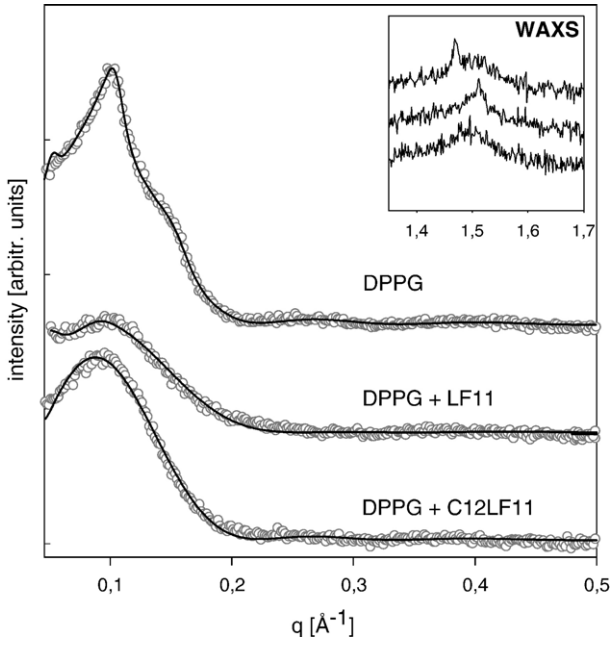

Fig. 3. SAXS- and WAXS-pattern (inset) of DPPG at 25 °C in the absence and presence of either LF11 or C12LF11, where grey circles represent experimental data and lines the calculated data. For clarity, the diffractograms are displaced on the ordinate by arbitrary units.

Table 3
Effect of LF11 and C12LF11 on the phosphorus–phosphorus distance (d_{pp}) of DPPG in the gel (25 °C) and fluid (50 °C) phase and DPPC in the gel phase (25 °C)

Temperature (°C)	Sample	d_{pp} (Å)
25	DPPG	44.4
	+LF11 (25:1)[a]	41.1
	+C12LF11 (25:1)	44.7
50	DPPG	37.0
	+LF11 (25:1)	36.5
	+C12LF11 (25:1)	37.8
25	DPPC	44.4
	+LF11 (25:1)	43.4
	+C12LF11 (25:1)	45.1

[a] Lipid to peptide molar ratio.

weakly correlated. This is due to electrostatic repulsion between the charged bilayers, which are only partially shielded by the sodium ions of the buffer. The bilayer itself is characterized by a d_{pp} distance of 44.4 Å (Table 3) in agreement with previous data [41]. The wide-angle X-ray pattern (Fig. 3, inset) shows a sharp reflection at 4.26 Å [39] and a shoulder at 4.15 Å, indicating a tilt of the hydrocarbon chains towards nearest neighbours [42]. Above T_m, at 50 °C (data not shown), the SAXS pattern shows broad diffuse scattering indicating a loss of positional correlation between the layers [43].

Addition of LF11 (25:1 lipid to peptide molar ratio) (Fig. 3) leads to a minor increase of the *d*-spacing (120 Å), but to a significant increase of the half-width of the Bragg peak, such that only the second order reflection can be observed. This indicates a further loss of positional correlations, seen also in the decrease of the domain size to 438 Å. A global fit to the scattering data further yielded a decrease of d_{pp} to 41.1 Å compared to pure DPPG. The SAXS pattern in the fluid phase (50 °C, data not shown) was typical for a bilayer transform characterized by a diffuse scattering. The calculated d_{pp} in the fluid phase exhibited no such significant changes between pure DPPG and in the presence of LF11 (37 vs. 36.5 Å, Table 3). In the wide-angle region, DPPG liposomes with LF11 showed a single relative sharp peak at 4.15 Å below the T_m characteristic for a hexagonal packing of the hydrocarbon chains, i.e., the tilt is lost. This may also explain the strong reduction of the pre-transition observed by DSC (Fig. 1).

The SAXS pattern in the gel phase in the presence of C12LF11 (25:1 lipid to peptide molar ratio) shows a complete loss of the positional correlations between the bilayers (Fig. 3) and the pattern corresponds to the Fourier transform of a single bilayer [34]. The derived d_{pp} value of 44.7 Å shows no significant change as compared to pure DPPG (Table 3). Addition of C12LF11 induced similar changes to the hydrocarbon chain packing as observed for LF11. Again, a single Bragg peak at 4.19 Å is detected in the wide-angle region (Fig. 3 inset), indicating a slightly decreased packing density as compared to LF11. Further, the increase of the peak width suggests a loss of correlation between the hydrocarbon chains. This is in accordance with DSC results (strongly reduced ΔH_m, low cooperativity) which also suggest loss of order of the hydrocarbon chain packing in the gel phase.

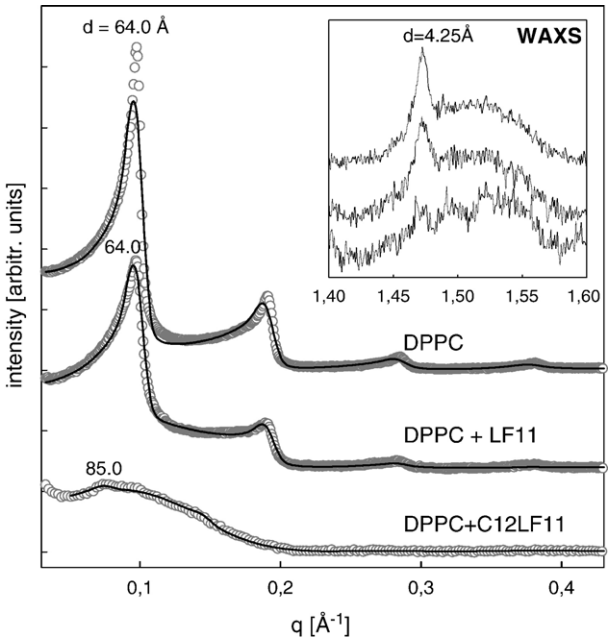

Fig. 4. SAXS- and WAXS-pattern (inset) of DPPC at 25 °C in the absence and presence of either LF11 or C12LF11, where grey circles represent experimental data and lines the calculated data. For clarity, the diffractograms are displaced on the ordinate by an arbitrary increment.

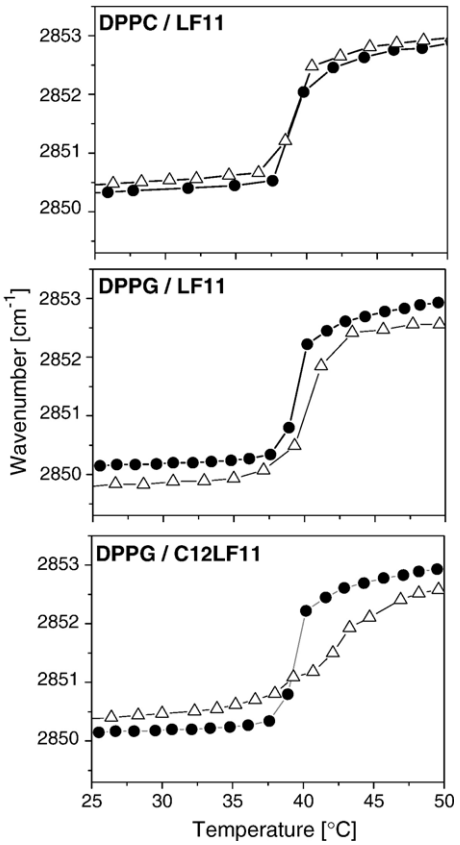

Fig. 5. Effect of LF11 and C12LF11 (lipid to peptide molar ratio of 5:1) on the main transition of DPPG and DPPC vesicles monitored by the peak position of the symmetric stretching vibration of the methylene groups of the lipids acyl chains. Full symbols correspond to pure lipids and open symbols to samples containing the respective peptide.

Table 4
Stern–Volmer quenching constant (K_{SV}) of LF11 and C12LF11 in PBS and DPPG membranes, respectively, and maxima of emission wavelength ($\lambda_{em,\ max}$) at a lipid to peptide molar ratio of 25:1

Peptide	K_{SV} in PBS [M^{-1}] ($\lambda_{em,\ max}$)	K_{SV} in DPPG liposomes [M^{-1}] ($\lambda_{em,\ max}$)
LF11	38.2 (352 nm)	5.0 (334 nm)
C12LF11	8.9 (339 nm)	3.6 (330 nm)

Small-angle X-ray scattering patterns of pure DPPC liposomes (Fig. 4) showed sharp Bragg reflections up to the 5th order indicating the existence of multilamellar vesicles [44]. A lamellar repeat distance (d-spacing) of 64 Å was calculated for the gel phase and 68 Å for the fluid phase (data not shown) in accordance with published data [45]. The d_{pp} was 44.4 Å, whereas the maximum domain size of 1600 Å was resolution limited, indicating that there are more than 25 bilayer stacks. The wide-angle pattern (Fig. 4 inset) shows similar to DPPG a sharp reflection at 4.25 Å and a broad shoulder indicative of a L_β-phase with hydrocarbon side-chains tilted relative to the normal of the bilayer plane [42].

Addition of LF11 did not markedly affect neither the wide-angle nor the small-angle X-ray scattering pattern (Fig. 4). There was no alteration of the peak position (d=64 Å) and a negligible effect on d_{pp} (43.4 Å). Only a slight broadening of the Bragg peaks was observed, suggesting a decrease of number of lamellae per scattering domain due to the presence of the peptide, which was confirmed by global analysis yielding a decrease of domain size to 960 Å, which corresponds to a stack of 15 bilayers.

In contrast, addition of C12LF11 dramatically affected the small-angle and wide-angle scattering pattern indicating a strong loss of positional correlations between layers and of hydrocarbon chain packing and therefore a major disturbance of membrane packing by the peptide. The position of the first order Bragg peak was displaced to 85 Å, superimposed on a broad diffuse scattering curve. The d_{pp} of 45.1 Å was not significantly altered, whereas the domain size was further decreased to 850 Å (stack of 10 bilayers) The strong diffuse background is in the present case most likely due to a large number of positionally uncorrelated bilayers, such as unilamellar vesicles. WAXS showed a completely different pattern now exhibiting a broad diffuse Bragg peak localized around 4.2 Å (Fig. 4 inset) characteristic for a bilayer with low order of hydrocarbon chain packing, again in agreement with DSC results.

3.4. FTIR spectroscopy

The variation of the peak position of the symmetric stretching vibration $\nu_s(CH_2)$ was monitored as a function of temperature through the main phase transition of DPPG and DPPC in the absence and presence LF11 and C12LF11, respectively (lipid to peptide molar ratio of 5:1). Addition of LF11 to DPPG (Fig. 5 middle) did not change significantly T_m as also observed in DSC, but induces a clear decrease in the wavenumber of the symmetric stretching vibration of the methylene groups of the DPPG acyl chains in the gel as well as fluid phase. This indicates a rigidification of the bilayer in both phases. Furthermore, LF11 has a pronounced reducing effect on the intensity of the anti-symmetric stretching vibration of the negatively charged phosphate group of DPPG (not shown), indicating its partial immobilization and thus interaction of LF11 with the DPPG head group. C12LF11 (bottom) broadened the phase transition range and exhibited an effect similar to cholesterol in phospholipid membranes [46]. The peptide enhanced namely the fluidity of the acyl chains in the gel phase (higher wavenumbers), but decreased it in the L_α phase (lower wavenumbers) (Fig. 5).

LF11 at a lipid to peptide molar ratio of 5:1 does neither affect the transition curve of DPPC nor the wavenumbers (Fig. 5 top) showing that there is no essential interaction between the peptide and lipid bilayer in accordance with DSC and X-ray

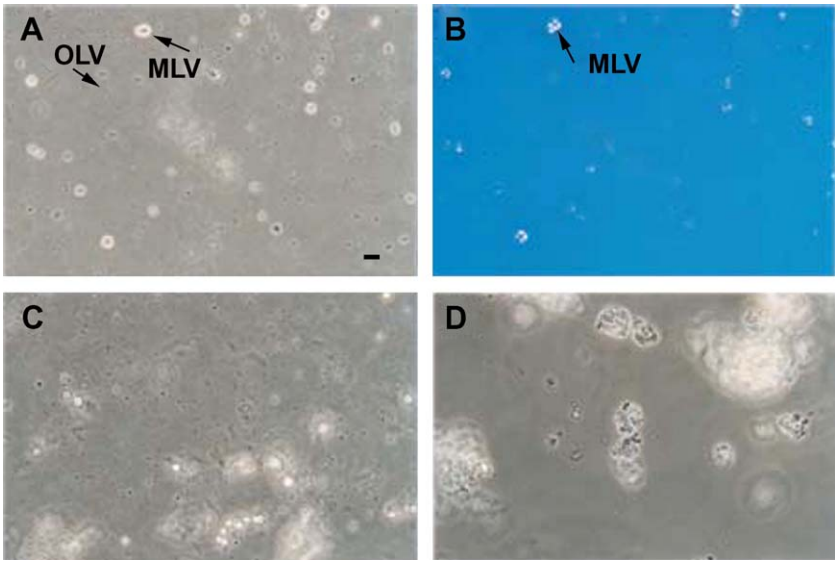

Fig. 6. Light microscopy of DPPG vesicles without (A) and with polarization filter (B) and in the presence of LF11 (C) or C12LF11 (D) at a lipid to peptide molar ratio of 25:1; Scale bar represents 10 μm.

data. In contrast, addition of C12LF11 on DPPC (data not shown) causes a reduction of T_m and broadens the phase transition range especially at higher peptide concentrations in agreement with DSC results. However, in contrast to DPPG liposomes the wavenumbers were not significantly affected.

3.5. Fluorescence spectroscopy

The K_{SV} in buffer provides an insight into the peptide solubility, translating to aggregation, whereas the K_{SV} in lipid environment together with the shift of the maxima of the respective emission wavelengths ($\lambda_{em,\ max}$ for pure Trp 353 nm [47]) provides insight into the depth of penetration of the single Trp of the peptide into the membrane.

As shown in Table 4 analysis of acrylamide-quenching of LF11 in PBS in the absence of lipid gave a Stern–Volmer constant (K_{SV}) of 38 M^{-1}. This suggests a complete exposure of tryptophan at position 3 of the peptide to the polar environment which demonstrates the absence of peptide aggregation. The corresponding value for C12LF11 in PBS at the same concentration is 9. This gives evidence for a lesser exposure of tryptophan to the polar environment and, in turn, potential aggregation of C12LF11. Addition of different amounts of the quencher acrylamide to DPPG-liposomes containing LF11 (lipid to peptide molar ratio of 25:1) gave a K_{SV} of 5 M^{-1} and a blue shift from 352 to 335 nm indicating a more hydrophobic environment for the tryptophan residue in the presence of DPPG than in buffer. A plausible explanation could be the change of secondary structure due to the presence of the negatively charged lipid that induces a peptide fold with a T-shaped arrangement of a hydrophobic core, formed by Phe^1, Trp^3 and Ile^7, and two clusters of basic residues [48]. Moreover, LF11 may to some extent dip into the bilayer interface as suggested from the FTIR experiments being in accordance with the reduced accessibility by the quencher molecule. An even lesser accessibility by acrylamide and stronger hydrophobic environment of Trp was observed for C12LF11, when added to DPPG liposomes. The quenching experiments yield a K_{SV} of 3.6 M^{-1} and a blue shift from 339 to 330 nm was observed. Both parameters are characteristic of an increase of the non polar environment of the tryptophan residue and indicate a stronger penetration of the peptide into the hydrophobic core of the DPPG membrane.

3.6. Optical microscopy

As can be seen in Fig. 6A the preparation of DPPG vesicles in PBS diluted from the X-ray samples to a concentration of 50 μg/ml gave predominantly OLVs (oligolamellar vesicles) (dark little dots) up to 1 μm and some MLVs (multilamellar vesicles) in the size range of 10 μm. Some bright spots may indicate the existence of ULVs (unilamellar vesicles). MLVs can be clearly observed as Maltese crosses under crossed polarizers (Fig. 6B). It has to be emphasized that the distribution of vesicles is not representative since MLVs are heavier and will therefore be more concentrated in the lower regions of the sample chamber, the field of observation. Addition of the peptides LF11 (Fig. 6C) and C12LF11 (Fig. 6D) to DPPG results in strong reduction of MLVs. These observations correlate with our X-ray-data. In case of LF11 some aggregated vesicles were observed, while in the presence of C12LF11 basically all vesicles found are aggregates, with aggregate sizes of up to 50 μm.

4. Discussion

Electrostatic interactions between a cationic peptide and anionic phospholipids initially favor binding of the peptide to the membrane surface, which is the generally agreed hypothesis concerning antimicrobial peptide selectivity [23]. This is also reflected in the biophysical studies on the interaction of LF11 with negatively charged DPPG and zwitterionic DPPC bilayers, respectively. The calorimetric, X-ray and FTIR data demonstrate that DPPC membranes remain unperturbed by LF11 showing that this peptide does not interact with this bilayer in accordance with the non-hemolytic activity of LF11. On the other hand, from the DSC thermograms, it is clear that although LF11 does not affect the main transition of DPPG liposomes appreciably, both in terms of enthalpy and transition temperature, the enthalpy of the pretransition is reduced by 80%. This indicates the occurrence of interference of the peptide with DPPG bilayers in agreement with observations from X-ray scattering, fluorescence and FTIR experiments. The latter shows that the peptide binds to the phosphate of the lipid headgroup, which is consistent with acrylamide quenching experiments that give evidence that the tryptophan residue is buried at least in the interface of the bilayer. Furthermore, X-ray data indicate a slight but significant thinning of the membrane in the gel phase as deduced from the reduced P–P distance in the presence of LF11 going hand in hand with a rearrangement of the hydrocarbon chains and a rigidification of these chains as seen by FTIR spectroscopy.

Membrane thinning was also observed upon addition of other antimicrobial peptides to lipid bilayers such as e.g., PGLa [44], melittin [49], alamethicin [50], magainin-2 [51], or MSI-78 [52]. They all have in common that the peptides induce a membrane thinning of 1–3 Å, which Ludtke et al. [51] explained by the adsorption of peptide molecules to the headgroup region that forces a gap in the chain region to be filled where the membrane must become locally thinner. In their model they approximate this as uniform thinning over the entire membrane. Mecke at al. [52] also supposed that MSI-78, an anologue of magainin-2, binds to DMPC bilayers forming distinct domains with in places (not uniform) reduction of bilayer thickness up to 11 Å. So it is conceivable that insertion of LF11 into the negatively charged membrane on the one side of the bilayer induces such a gap that is compensated by the hydrophobic chains of the opposite monolayers of the bilayer causing the observed overall membrane thinning. Nevertheless the antimicrobial activity of LF11 is weak, which may be due to the low overall hydrophobicity of the peptide.

Using combinatorial libraries analogs of a cationic amphipathic peptide were identified in which hydrophobic residues inserted into the hydrophilic face have resulted in a greater

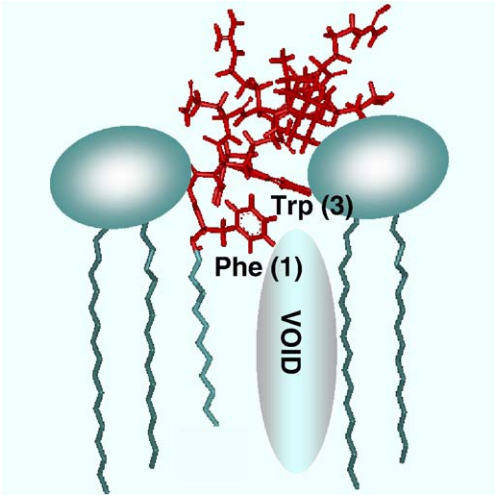

Fig. 7. Schematic representation of insertion of C12LF11 into DPPC membranes indicating the void formed within the hydrophobic core of the bilayer. Lipid and peptide are to scale, whereby the peptide structure is based on NMR data (manuscript in preparation).

therapeutic index than the original peptide [23,53]. Similarly, acylation of weakly or inactive peptides may compensate for lack of hydrophobicity [24] and favor membrane insertion and thus membrane permeation [54,55]. In fact, some potent antimicrobial peptides of bacterial and fungal origin like echinicandin [56], polmyxins [57], or daptomycin [58] contain fatty acids. It has been postulated that acylation of proteins helps to increase their membrane association and sorting into specific subcellular localization [56,59]. Furthermore, reports have shown that removal of the acyl chain of polymyxin B causes a decrease in its LPS-neutralizing potency and lower antimicrobial activities [60–62]. This suggests that addition of an acyl chain to an antimicrobial peptide should result in stronger antimicrobial activity. In fact, several studies to assess the effect of acylation have demonstrated that conjugation of fatty acids to cationic peptides enhances their antimicrobial activity [25,54,63–65].

This was also observed upon N-acylation of LF11 that dramatically enhanced the effect of the peptide as shown in the biological activity assays as well as in membrane model systems. However, as can be deduced from the obtained data, C12LF11 is now able to penetrate the membrane independently on the charge of the headgroup, although binding and depth of membrane penetration of C12LF11 may vary depending on the nature of the phospholipid headgroup. Hydrogen exchange protection in NMR experiments showed that in anionic micelles LF11 is less deeply inserted into the hydrophobic core than in zwitterionic micelles indicating the decreasing extent of insertion of the N terminus and potential role of peptide plasticity in differentiation between bacterial and eukaryotic membranes [48]. Nevertheless, the lauryl group of the peptide will penetrate into the hydrophobic core of the membrane strongly perturbing the lipid packing of both DPPG and DPPC bilayers. A loss of chain correlation is evident from the wide-angle X-ray pattern as well as reduction of ΔH_m. The decrease of T_m further indicates the destabilization of the gel phase. These observations can be explained by the creation of voids in the hydrophobic core of the membrane as schematically shown in Fig. 7. This can arise due to both the hydrophobic mismatch of the acyl chains of the peptide (C_{12}) and lipids (C_{16}), as has been described for the interaction of small amphipathic molecules such as fatty acids or detergents [66], and the insertion of the hydrophobic amino acid cluster (Phe^1, Trp^3) in the membrane interface. This is energetically an unfavorable situation and hence the system will rearrange in a way that hydrophobic interactions are maximized, i.e., by disordering of the hydrocarbon chains to fill the void. Although DSC and X-ray studies showed the same effects of C12LF11 on both membrane model systems, FTIR spectroscopy experiments indicated some differences in the kind of perturbation of the hydrocarbon chains. While the rigidity of the acyl chains of DPPC was not markedly affected by C12LF11, a cholesterol like effect (increase of fluidity below and a decrease of fluidity above T_m) was observed for the C12LF11/DPPG system. This may be explained by a different structural arrangement of the N-lauryl chain, when inserted into zwitterionic or negatively charged membrane systems. Indeed 2D-NMR experiments revealed that in zwitterionic DPC (dodecylphosphocholine) micelles the structure of the N-acyl chain was not well defined, while in negatively charged SDS micelles, the hydrophobic chain makes a sharp turn towards the peptide backbone (manuscript in preparation). Such a bend structure of the N-lauryl chain together with the aromatic residues of Phe^1 and Trp^3 could mimic to some extent the rigid ring structure of cholesterol.

Pre-assembly of the acylated peptide in solution as indicated by fluorescence spectroscopy experiments may also be a factor for the unspecific interaction between C12LF11 and membrane model systems as suggested earlier [67]. For example, covalently linked pentameric bundles of diastereomeric cationic peptides exhibited independent on the peptide length (13,16,19 amino acid residues) high activity towards fungi, bacteria and red blood cells, while the monomeric peptides showed length-dependent antimicrobial activity and were devoid of hemolytic activity [68].

Thus, electrostatic interactions seem to play an important role for the membrane binding of the peptide but for penetration a certain threshold value of hydrophobicity is needed, which results in a stronger membrane perturbation. This is in accordance with the great difference in activity observed between LF11 and C12LF11. However, as described e.g., for PGLa [69], membrane selectivity is caused predominantly by electrostatic attraction of the peptide to the membrane surface and not by hydrophobic insertion. Therefore, a certain balance within electrostatic interaction and hydrophobicity is required for specific and high activity towards bacterial membranes [10], which has also been shown for other lipopeptides [24] and will be a challenge for the future.

Acknowledgements

This study has been carried out with the financial support from the Commission of the European Communities, specific

RTD programme "Quality of Life and Management of Living Resources", QLK2-CT-2002-01001, "Antimicrobial endotoxin neutralizing peptides to combat infectious diseases". R. Jerala was also supported by the Slovenian Research Agency. We thank G. von Busse for performing the FTIR measurements.

References

[1] K. Lohner, E. Staudegger, Are we on the threshold of the post-antibiotic era? in: K. Lohner (Ed.), Development of Novel Antimicrobial Agents: Emerging Strategies, Horizon Scientific Press, Wymondham, Norfolk, UK, 2001, pp. 1–15.
[2] M. Zasloff, Antibiotic peptides as mediators of innate immunity, Curr. Opin. Immunol. 4 (1992) 3–7.
[3] M.G. Scott, R.E. Hancock, Cationic antimicrobial peptides and their multifunctional role in the immune system, Crit. Rev. Immunol. 20 (2000) 407–431.
[4] W. Kamysz, Are antimicrobial peptides an alternative for conventional antibiotics? Nucl. Med. Rev. Cent. East Eur. 8 (2005) 78–86.
[5] R.M. Epand, H.J. Vogel, Diversity of antimicrobial peptides and their mechanisms of action, Biochim. Biophys. Acta 1462 (1999) 11–28.
[6] K. Lohner, E.J. Prenner, Differential scanning calorimetry and X-ray diffraction studies of the specificity of the interaction of antimicrobial peptides with membrane-mimetic systems, Biochim. Biophys. Acta 1462 (1999) 141–156.
[7] K. Lohner, The role of membrane lipid composition in cell targeting and their mechanism of action, in: K. Lohner (Ed.), Development of Novel Antimicrobial Agents: Emerging Strategies, Horizon Scientific Press, Wymondham, Norfolk, U.K, 2001, pp. 149–165.
[8] K. Matsuzaki, K. Sugishita, N. Fujii, K. Miyajima, Molecular basis for membrane selectivity of an antimicrobial peptide, magainin 2, Biochemistry 34 (1995) 3423–3429.
[9] K.J. Hallock, D.K. Lee, J. Omnaas, H.I. Mosberg, A. Ramamoorthy, Membrane composition determines pardaxin's mechanism of lipid bilayer disruption, Biophys. J. 83 (2002) 1004–1013.
[10] K. Lohner, S.E. Blondelle, Molecular mechanisms of membrane perturbation by antimicrobial peptides and the use of biophysical studies in the design of novel peptide antibiotics, Comb. Chem. High Throughput Screen. 8 (2005) 241–256.
[11] H.J. Vogel, D.J. Schibli, W. Jing, E.M. Lohmeier-Vogel, R.F. Epand, R.M. Epand, Towards a structure–function analysis of bovine lactoferricin and related tryptophan- and arginine-containing peptides, Biochem. Cell Biol. 80 (2002) 49–63.
[12] J.L. Gifford, H.N. Hunter, H.J. Vogel, Lactoferricin: a lactoferrin-derived peptide with antimicrobial, antiviral, antitumor and immunological properties, Cell Mol. Life Sci. 62 (2005) 2588–2598.
[13] M. Sorenson, M.P.L. Sorenson, The proteins in whey, C.R. Trav. Lab. Carlsberg 23 (1939) 55–59.
[14] P.L. Masson, J.F. Heremans, E. Schonne, Lactoferrin, an iron-binding protein in neutrophilic leukocytes, J. Exp. Med. 130 (1969) 643–658.
[15] P.L. Masson, J.F. Heremans, C.H. Dive, An iron binding protein common to many external secretions, Clin. Chim. Acta 14 (1966) 735–739.
[16] E.W. Odell, R. Sarra, M. Foxworthy, D.S. Chapple, R.W. Evans, Antibacterial activity of peptides homologous to a loop region in human lactoferrin, FEBS Lett. 382 (1996) 175–178.
[17] P.M. Hwang, N. Zhou, X. Shan, C.H. Arrowsmith, H.J. Vogel, Three-dimensional solution structure of lactoferricin B, an antimicrobial peptide derived from bovine lactoferrin, Biochemistry 37 (1998) 4288–4298.
[18] W. Bellamy, M. Takase, H. Wakabayashi, K. Kawase, M. Tomita, Antibacterial spectrum of lactoferricin B, a potent bactericidal peptide derived from the N-terminal region of bovine lactoferrin, J. Appl. Bacteriol. 73 (1992) 472–479.
[19] H.N. Hunter, A.R. Demcoe, H. Jenssen, T.J. Gutteberg, H.J. Vogel, Human lactoferricin is partially folded in aqueous solution and is better stabilized in a membrane mimetic solvent, Antimicrob. Agents Chemother. 49 (2005) 3387–3395.
[20] H. Wakabayashi, M. Takase, M. Tomita, Lactoferricin derived from milk protein lactoferrin, Curr. Pharm. Des. 9 (2003) 1277–1287.
[21] M. Dathe, M. Schumann, T. Wieprecht, A. Winkler, M. Beyermann, E. Krause, K. Matsuzaki, O. Murase, M. Bienert, Peptide helicity and membrane surface charge modulate the balance of electrostatic and hydrophobic interactions with lipid bilayers and biological membranes, Biochemistry 35 (1996) 12612–12622.
[22] M. Dathe, H. Nikolenko, J. Meyer, M. Beyermann, M. Bienert, Optimization of the antimicrobial activity of magainin peptides by modification of charge, FEBS Lett. 501 (2001) 146–150.
[23] S.E. Blondelle, K. Lohner, Combinatorial libraries: a tool to design antimicrobial and antifungal peptide analogues having lytic specificities for structure–activity relationship studies, Biopolymers 55 (2000) 74–87.
[24] D. Avrahami, Y. Shai, A new group of antifungal and antibacterial lipopeptides derived from non-membrane active peptides conjugated to palmitic acid, J. Biol. Chem. 279 (2004) 12277–12285.
[25] H. Wakabayashi, H. Matsumoto, K. Hashimoto, S. Teraguchi, M. Takase, H. Hayasawa, N-Acylated and D enantiomer derivatives of a nonamer core peptide of lactoferricin B showing improved antimicrobial activity, Antimicrob. Agents Chemother. 43 (1999) 1267–1269.
[26] M.B. Strom, B.E. Haug, O. Rekdal, M.L. Skar, W. Stensen, J.S. Svendsen, Important structural features of 15-residue lactoferricin derivatives and methods for improvement of antimicrobial activity, Biochem. Cell Biol. 80 (2002) 65–74.
[27] S.E. Blondelle, K. Lohner, M. Aguilar, Lipid-induced conformation and lipid-binding properties of cytolytic and antimicrobial peptides: determination and biological specificity, Biochim. Biophys. Acta 1462 (1999) 89–108.
[28] A. Majerle, J. Kidric, R. Jerala, Enhancement of antibacterial and lipopolysaccharide binding activities of a human lactoferrin peptide fragment by the addition of acyl chain, J. Antimicrob. Chemother. 51 (2003) 1159–1165.
[29] J. Andrä, K. Lohner, S.E. Blondelle, R. Jerala, I. Moriyon, M.H. Koch, P. Garidel, K. Brandenburg, Enhancement of endotoxin neutralization by coupling of a C12-alkyl chain to a lactoferricin-derived peptide, Biochem. J. 385 (2005) 135–143.
[30] B.J. Appelmelk, Y.Q. An, M. Geerts, B.G. Thijs, H.A. de Boer, D.M. MacLaren, J. de Graaff, J.H. Nuijens, Lactoferrin is a lipid A-binding protein, Infect. Immun. 62 (1994) 2628–2632.
[31] F.L. Hahn, R. Luckhaus, Ein vorzügliches Reagenz zur kolorimetrischen Bestimmung von Phosphat und Arsenat, Z. Anal. Chem. 149 (1956) 172–177.
[32] S.E. Blondelle, E. Takahashi, P.A. Weber, R.A. Houghten, Identification of antimicrobial peptides by using combinatorial libraries made up of unnatural amino acids, Antimicrob. Agents Chemother. 38 (1994) 2280–2286.
[33] P. Laggner, H. Mio, Swax—A dual-detector camera for simultaneous small-angle and wide-angle X-ray-diffraction in polymer and liquid-crystal research, Nucl. Instrum. Methods Phys. Res. 323 (1992) 86–90.
[34] G. Pabst, R. Koschuch, B. Pozo-Navas, M. Rappolt, K. Lohner, P. Laggner, Structural analysis of weakly ordered membrane stacks, J. Appl. Crystallogr. 36 (2003) 1378–1388.
[35] G. Pabst, M. Rappolt, H. Amenitsch, P. Laggner, Structural information from multilamellar liposomes at full hydration: full q-range fitting with high quality X-ray data, Phys. Rev., E Stat. Phys. Plasmas Fluids Relat. Interdiscip. Topics 62 (2000) 4000–4009.
[36] J.B. Birks (Ed.), Photophysics of Aromatic Molecules, Wiley-Interscience, 1970, pp. 433–447.
[37] T. Tao, J. Cho, Fluorescence lifetime quenching studies on the accessibilities of actin sulfhydryl sites, Biochemistry 18 (1979) 2759–2765.
[38] K.K. Eklund, I.S. Salonen, P.K. Kinnunen, Monovalent cation dependant phase behaviour of dipalmitoylglycerol, Chem. Phys. Lipids. 50 (1989) 71–78.
[39] A. Latal, G. Degovics, R.F. Epand, R.M. Epand, K. Lohner, Structural aspects of the interaction of peptidyl-glycylleucine-carboxyamide, a highly

potent antimicrobial peptide from frog skin, with lipids, Eur. J. Biochem. 248 (1997) 938–946.
[40] R. Koynova, M. Caffrey, Phases and phase transitions of the phosphatidylcholines, Biochim. Biophys. Acta 1376 (1998) 91–145.
[41] G. Degovics, A. Latal, K. Lohner, X-ray studies on aqueous dispersions of dipalmitoyl phosphatidylglycerol in the presence of salt, J. Appl. Crystallogr. 33 (2000) 544–547.
[42] A. Tardieu, V. Luzzati, F.C. Reman, Structure and polymorphism of the hydrocarbon chains of lipids: a study of lecithin–water phases, J. Mol. Biol. 75 (1973) 711–733.
[43] B. Pozo-Navas, V.A. Raghunathan, J. Katsaras, M. Rappolt, K. Lohner, G. Pabst, Discontinuous unbinding of lipid multibilayers, Phys. Rev. Lett. 91 (2003) 028101(1)–028101(4).
[44] P. Laggner, K. Lohner, Liposome phase systems as membrane activity sensors for peptides, in: J. Katsaras, T. Gutberlet (Eds.), Lipid Bilayers. Structure and Interactions, Springer-Verlag, 2000, pp. 233–264.
[45] J.F. Nagle, S. Tristram-Nagle, Structure of lipid bilayers, Biochim. Biophys. Acta 1469 (2000) 159–195.
[46] J.C. Owicki, H.M. Mcconnell, Theory of protein–lipid and protein–protein interactions in bilayer membranes, Proc. Natl. Acad. Sci. U. S. A. 76 (1979) 4750–4754.
[47] J.R. Lakowicz, Principles of Fluorescence Spectroscopy, Kluwer Academic/Plenum Publishers, New York, 1999.
[48] B. Japelj, P. Pristovsek, A. Majerle, R. Jerala, Structural origin of endotoxin neutralization and antimicrobial activity of a lactoferrin-based peptide, J. Biol. Chem. 280 (2005) 16955–16961.
[49] F.Y. Chen, M.T. Lee, H.W. Huang, Evidence for membrane thinning effect as the mechanism for peptide-induced pore formation, Biophys. J. 84 (2003) 3751–3758.
[50] K. He, S.J. Ludtke, W.T. Heller, H.W. Huang, Mechanism of alamethicin insertion into lipid bilayers, Biophys. J. 71 (1996) 2669–2679.
[51] S. Ludtke, K. He, H. Huang, Membrane thinning caused by magainin 2, Biochemistry 34 (1995) 16764–16769.
[52] A. Mecke, D.K. Lee, A. Ramamoorthy, B.G. Orr, M.M. Banaszak Holl, Membrane thinning due to antimicrobial peptide binding: an atomic force microscopy study of MSI-78 in lipid bilayers, Biophys. J. 89 (2005) 4643–4650.
[53] S.E. Blondelle, R.A. Houghten, Novel antimicrobial compounds identified using synthetic combinatorial library technology, Trends Biotechnol. 14 (1996) 60–65.
[54] P. Mak, J. Pohl, A. Dubin, M.S. Reed, S.E. Bowers, M.T. Fallon, W.M. Shafer, The increased bactericidal activity of a fatty acid-modified synthetic antimicrobial peptide of human cathepsin G correlates with its enhanced capacity to interact with model membranes, Int. J. Antimicrob. Agents 21 (2003) 13–19.
[55] S. Thennarasu, D.K. Lee, A. Tan, K.U. Prasad, A. Ramamoorthy, Antimicrobial activity and membrane selective interactions of a synthetic lipopeptide MSI-843, Biochim. Biophys. Acta 1711 (2005) 49–58.
[56] D.W. Denning, Echinocandins and pneumocandins—A new antifungal class with a novel mode of action, J. Antimicrob. Chemother. 40 (1997) 611–614.
[57] I. Ofek, S. Cohen, R. Rahmani, K. Kabha, D. Tamarkin, Y. Herzig, E. Rubinstein, Antibacterial synergism of polymyxin B nonapeptide and hydrophobic antibiotics in experimental gram-negative infections in mice, Antimicrob. Agents Chemother. 38 (1994) 374–377.
[58] W.E. Alborn Jr., N.E. Allen, D.A. Preston, Daptomycin disrupts membrane potential in growing *Staphylococcus aureus*, Antimicrob. Agents Chemother. 35 (1991) 2282–2287.
[59] M.D. Resh, Fatty acylation of proteins: new insights into membrane targeting of myristoylated and palmitoylated proteins, Biochim. Biophys. Acta 1451 (1999) 1–16.
[60] M. Vaara, Agents that increase the permeability of the outer membrane, Microbiol. Rev. 56 (1992) 395–411.
[61] F. Rose, K.U. Heuer, U. Sibelius, S. Hombach-Klonisch, L. Kiss, W. Seeger, F. Grimminger, Targeting lipopolysaccharides by the nontoxic polymyxin B nonapeptide sensitizes resistant *Escherichia coli* to the bactericidal effect of human neutrophils, J. Infect. Dis. 182 (2000) 191–199.
[62] H. Tsubery, I. Ofek, S. Cohen, M. Fridkin, Structure–function studies of polymyxin B nonapeptide: implications to sensitization of gram-negative bacteria, J. Med. Chem. 43 (2000) 3085–3092.
[63] N.A. Lockwood, J.R. Haseman, M.V. Tirrell, K.H. Mayo, Acylation of SC4 dodecapeptide increases bactericidal potency against Gram-positive bacteria, including drug-resistant strains, Biochem. J. 378 (2004) 93–103.
[64] A.F. Chu-Kung, K.N. Bozzelli, N.A. Lockwood, J.R. Haseman, K.H. Mayo, M.V. Tirrell, Promotion of peptide antimicrobial activity by fatty acid conjugation, Bioconjugate Chem. 15 (2005) 530–535.
[65] D. Avrahami, Y. Shai, Bestowing antifungal and antibacterial activities by lipophilic acid conjugation to D,L-amino acid-containing antimicrobial peptides: a plausible mode of action, Biochemistry 42 (2003) 14946–14956.
[66] K. Lohner, Effects of small organic molecules on phospholipid phase transitions, Chem. Phys. Lipids 57 (1991) 341–362.
[67] J. Strahilevitz, A. Mor, P. Nicolas, Y. Shai, Spectrum of antimicrobial activity and assembly of dermaseptin-b and its precursor form in phospholipid membranes, Biochemistry 33 (1994) 10951–10960.
[68] N. Sal-Man, Z. Oren, Y. Shai, Preassembly of membrane-active peptides is an important factor in their selectivity toward target cells, Biochemistry 41 (2002) 11921–11930.
[69] T. Wieprecht, O. Apostolov, M. Beyermann, J. Seelig, Membrane binding and pore formation of the antibacterial peptide PGLa: thermodynamic and mechanistic aspects, Biochemistry 39 (2000) 442–452.